PERGAMON

Available online at www.sciencedirect.com
SCIENCE DIRECT®

Corrosion Science 45 (2003) 2043–2053

CORROSION SCIENCE

www.elsevier.com/locate/corsci

Soft X-ray absorption spectroscopy study of the effects of Si, Ce, and Mo ion implantation on the passive layer of AISI 304 stainless steel

M.F. López [a,*], A. Gutiérrez [b], F.J. Pérez [c], M.P. Hierro [c], F. Pedraza [c]

[a] *Instituto de Ciencia de Materiales de Madrid, CSIC, Cantoblanco, E-28049 Madrid 28040, Spain*
[b] *Departamento de Física Aplicada, Universidad Autónoma de Madrid, Cantoblanco, E-28049 Madrid, Spain*
[c] *Departamento de Ciencia de Materiales, Universidad Complutense de Madrid, Facultad Ciencias Químicas, Madrid 28040, Spain*

Received 22 April 2002; accepted 17 January 2003

Abstract

The chemical modifications introduced in the passive layer of AISI 304 stainless steel after Si, Ce, and Mo ion implantation were investigated and compared with non-implanted steel by soft X-ray absorption spectroscopy. The influence of ion implantation on the passive properties was evaluated by measuring soft X-ray absorption spectra at the Cr, Fe, Ni, Mn and Si 2p in addition to oxygen 1s thresholds. All ion implanted samples show a relative Cr-enrichment at the surface as compared with non-implanted samples. Fe 2p as well as O 1s spectral changes reveal chemical differences in the passive layer as a function of the element ion-implanted.

Keywords: A. Stainless steel; B. Ion implantation; C. Passive films

1. Introduction

Stainless steels (SSs) are materials with a high Cr-content which react easily with oxygen from the atmosphere, giving rise to a Cr_2O_3-rich film responsible for maintaining passivity. The passive film formed on these alloys is a mixture of iron and

* Corresponding author. Tel.: +34-91-3349000; fax: +34-91-3720623.
E-mail address: mflopez@icmm.csic.es (M.F. López).

0010-938X/03/$ - see front matter © 2003 Elsevier Science Ltd. All rights reserved.
doi:10.1016/S0010-938X(03)00029-5

chromium oxides, in which Cr is enriched compared to the bulk content. The enrichment in chromium is related to the stability of chromium oxide and its low mobility in the film. The presence and stability of the passive film on the material surface results in excellent corrosion behavior [1,2].

Nowadays several surface modification methods on conventional SSs, as well as chemical modifications on their composition, have been proposed to prolong the in-service lifetime of these materials [3,4]. In previous studies, the addition of some reactive elements (Ce, La, ...) that could improve the corrosion properties of the passive layers of these materials has been investigated [5–7]. Furthermore, the addition of Mo is known to increase the pitting corrosion resistance of SSs [8,9]. Additionally, SSs are materials of interest for elevated temperature applications [10]. The effects of these reactive element additions, which improve the high temperature oxidation behavior, have been also studied [5,6]. Furthermore, the addition of Si is expected to influence the oxidation behavior of these materials in a similar way to the reactive element addition [11].

Several established processes exist for introducing a low concentration of these reactive elements. One method is ion implantation, which allows metallic species and gases to be implanted into the surface region of materials to improve properties such as wear, erosion and corrosion [12,13]. Indeed, the material surface is the region that will be in contact with the aggressive environment and, therefore, the relevant region to be modified. Among the advantages of ion implantation is the modification of the surface without a significant change in the dimensions of the piece implanted, since the implantation profile corresponds only to a few hundred Angstroms. The depth will depend on the mass and energy of the implanted ion, and the concentration on the dose. Moreover, the bulk mechanical properties of the material remain unaffected [14].

The influence of ion implantation on the properties of the room temperature passive layer of SSs can be evaluated by investigating the surface chemical composition. The techniques most widely used to study SS surfaces have been X-ray photoelectron spectroscopy (XPS) and Auger electron spectroscopy (AES) [15–18]. Most of these scientific investigations have studied SSs after passivation in aqueous solution. The sampling depth of both surface analysis methods (XPS and AES) is about 20 Å [19]. Soft X-ray absorption spectroscopy (XAS) is particularly suited to determining the chemical state of the different species at the outer layer. Soft X-ray absorption is a local process in which an electron is promoted from a core state to an empty state. The absorption cross section is measured by detecting electrons, which escape from the surface after the decay of the core hole. In the total electron yield mode (TEY) all escaping electrons are detected. Although a consensus on the quantitative value of the probing depth of XAS in TEY has not been reached, previous studies indicate values around 40 Å or higher [20–22]. Therefore, XAS in TEY mode permits the study of the chemical composition of 20–30 Å thick passive films on SSs [23,24]. XAS is a technique that allows detailed element-specific studies because the core level binding energies are well defined for each chemical element. The case of the transition metal 2p thresholds corresponds to transitions from 2p to 3d orbitals at the transition metal sites. In this case, the XAS spectra will be influenced by interactions with the outer band electrons. XAS can be used to provide quantitative information because the absorption strength is proportional to the concentration of the corresponding element in the heterogeneous system.

The aim of the present study is to investigate the chemical effects of ion implantation of Si, Ce and Mo in AISI 304 SS, using soft XAS. By applying this technique at the metals 2p edges and at the O 1s edge in TEY mode it is possible to determine the main contributions to the composition of the passive layers formed spontaneously on the surface of these materials.

2. Experimental

Specimens of $15 \times 3.5 \times 1$ mm^3 austenitic AISI 304 SS with a nominal chemical composition of (wt%) 18.2 Cr, 9.4 Ni, 1.5 Mn, 0.4 Si, 0.2 Mo, 0.2 Cu, 0.1 Co, 0.047 C, 0.027 P, 0.005 N, 0.003 S, 0.003 Ti, 0.002 Al and balance Fe were investigated. Before testing, the samples were mechanically polished with SiC emery paper up to # 600, and then ultrasonically degreased in acetone.

Si, Mo and Ce ion implantation was carried out at an energy of 150 keV with ion doses of 1×10^{15} Si/cm^2, 1×10^{14} Mo/cm^2 and 1×10^{14} Ce/cm^2. The implantation profile was calculated by means of TRIM96 (Transport and Range of Ions in Matter [25,26]) computational code showing a projected range, R_p, that reached about 982 Å depth in the material for Si, about 358 Å for Mo and about 308 Å for Ce.

After the ion implantation process, the samples were exposed to air and stored in a dessicator for 36 days until they were placed in the ultrahigh vacuum chamber for the XAS measurements. For comparative purposes and as reference materials, the following samples were also studied: (a) as-received AISI 304 SS sample; (b) Fe and Cr pure metal samples, in the form of polycrystalline material (these samples were scraped in situ in the UHV chamber with a diamond file to expose and measure the clean metal surfaces), and (c) oxidized Fe and oxidized Cr samples. Both Fe and Cr oxidized samples were produced by room temperature air exposure of the metal samples, generating spontaneously a native oxide layer on each sample surface.

The XAS measurements were carried out at the PM-1 soft X-ray monochromator at the Berliner Elektronenspeicherring für Synchrotronstrahlung (BESSY). XAS spectra were obtained at the transition metals 2p absorption thresholds (Cr, Fe, Ni and Mn), the silicon 2p and the oxygen 1s absorption thresholds by recording the total yield of secondary electrons from the sample surfaces, i.e., in TEY mode. The base pressure in the UHV-chamber during the measurements was better than 2×10^{-10} mbar.

3. Results and discussion

Fig. 1 shows the percentage composition of the main elements of AISI 304 SS samples, i.e., non-implanted and Si, Ce and Mo ion implanted specimens, as

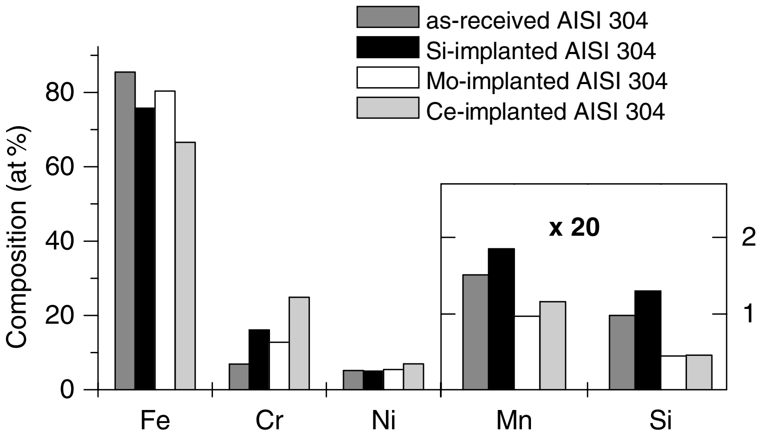

Fig. 1. Percentage composition of the as-received AISI 304 SS, and this material after Si, Ce and Mo ion implantation.

measured by XAS in this study. The values represented in this graph were obtained from the XAS spectra corresponding to the different absorption edges. Ce and Mo data are not shown because the Ce 3d and Mo 3p XAS signals were negligible. This result is a consequence of the depth profile of the implanted elements larger than the XAS probing depth. Since AISI 304 contains 0.4 wt% of Si, the Si 2p XAS signal was significant and the Si concentration could be calculated as it is shown in Fig. 1. The most significant result obtained from Fig. 1 is the high value obtained for Fe, taking into account that the passive layer of AISI 304 SS is expected to be mainly formed by Cr compounds. As the probing depth (around 40 Å or higher) is slightly higher than the film thickness (20–30 Å), the values obtained with XAS correspond not only to the passive film but also to the metallic substrate. For a more precise indication of the passive layer chemical composition it is essential to study the more relevant transition metal absorption threshold spectra.

Fig. 2 shows the Fe 2p soft X-ray absorption spectra for all of the AISI 304 SSs, i.e. the as-received, and the Si, Mo, and Ce ion implanted samples. They are compared with the spectra of Fe metal, oxidized Fe, Fe_2O_3 and Fe_3O_4, the three latter taken from Ref. [27]. All spectra consist of two multiplets, which are separated, to a first approximation, by the spin–orbit splitting of the Fe 2p core hole. The different Fe 2p spectral shapes obtained for the AISI 304 samples indicate that the ion implantation process causes chemical changes at the outer layers of the material. The Fe 2p spectrum of the as-received AISI 304 sample is similar to that of metallic Fe, although a spectral structure at $\approx$708 eV appears for the AISI 304 sample. The metallic contribution of the as-received AISI 304 Fe 2p spectrum indicates that the XAS signal has a component coming from the substrate. The spectral shoulder located at $\approx$708 eV could be assigned to a small amount of Fe oxides, as can be deduced by comparing it with the Fe_2O_3 and Fe_3O_4 spectra, which would increase the spectral structure at $\approx$708 eV [27].

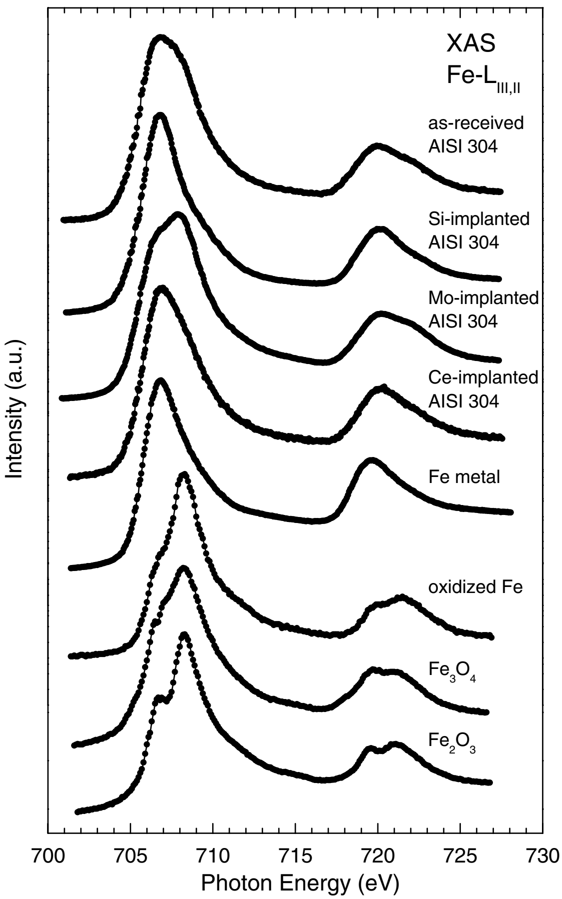

Fig. 2. Fe 2p soft X-ray absorption spectra of all AISI 304 SS samples, as-received and after Si, Mo, and Ce ion implantation, as well as Fe metal, oxidized Fe, Fe_2O_3 and Fe_3O_4 samples. The solid lines through the data points serve as a guide to the eyes.

The Si-implanted AISI 304 sample exhibits the typical Fe 2p spectrum of Fe metal, suggesting that the Fe signal is coming mainly from the substrate, and, therefore, in this sample almost no Fe oxides nor hydroxides are present in the passive layer. On the other hand, the shape of the Fe 2p Mo-implanted AISI 304 signal is rather different to the other AISI 304 samples. This XAS signal can be assigned to a mixture of metallic Fe and Fe oxides. In this case, since the main peak is located at $\approx$708 eV, the contribution of Fe oxides is rather high. Finally, the Fe 2p spectrum of the Ce-implanted AISI 304 sample exhibits mainly a signal corresponding to Fe metal as can be deduced from its similarity with the Fe metal spectrum. This result suggests that the signal is also coming from the substrate. However, the spectral shape is slightly broader than in Fe metal, with a more pronounced spectral feature at $\approx$708 eV, which may be assigned to a small amount of Fe oxides.

Therefore, although Fig. 1 suggests that Fe is the major component of the passive layer of AISI 304 SSs, this is not the case because, due to the probing depth of this technique, not all the Fe signal is coming from the passive layer. The Fe 2p XAS spectrum of the as-received AISI 304 sample exhibits Fe in metallic form with some amount of Fe_2O_3 and Fe_3O_4. In the Mo-implanted AISI 304 sample the spectrum exhibits both metallic Fe and Fe oxides with a high contribution of the latter. The Si and Ce ion implanted sample spectra show mainly Fe in metallic form, with Ce-containing sample passive layer having some amount of Fe oxides.

In Fig. 1, Cr was shown as the second important element of the chemical composition of the SS outer layers. Fig. 3 shows the Cr 2p soft X-ray absorption spectra of all AISI 304 SS samples as well as oxidized Cr, and Cr metal for comparison. All

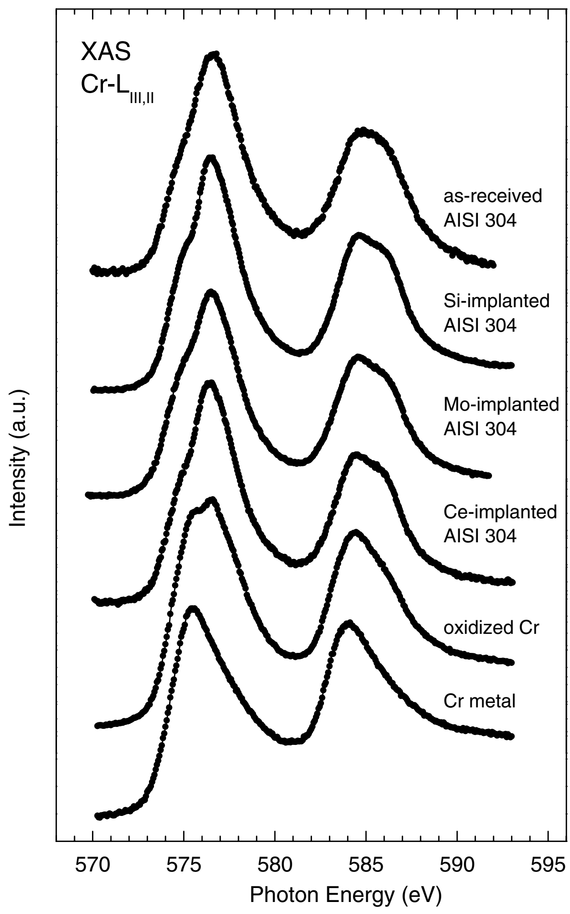

Fig. 3. Cr 2p soft X-ray absorption spectra of all AISI 304 SS samples: as-received and after Si, Mo, and Ce ion implantation, as well as oxidized Cr and Cr metal samples. The solid lines through the data points serve as a guide to the eyes.

spectra reveal two broad multiplets separated by the spin–orbit splitting of the Cr 2p core hole. The soft X-ray absorption spectrum of Cr_2O_3 exhibits a peak at ≈576.5 eV in the $2p_{3/2}$ region and a distinctive shoulder at ≈575 eV. The spectrum of Cr metal has a different shape than that of Cr_2O_3 with a peak located at ≈575 eV. The oxidized Cr spectrum that corresponds to the native oxide film is a mixture of metallic chromium and Cr_2O_3. The shoulder located at ≈575 eV is better defined in the spectrum of the Si-implanted AISI 304. This result suggests that the spectral width of the two peaks, shoulder and main structure is smaller for the Si-implanted AISI 304 sample than for the other samples, indicating the presence of a primary Cr_2O_3 oxide structure. This is corroborated by the Cr_2O_3 spectrum of previous work [27]. For the Mo-implanted, Ce-implanted, and as-received AISI 304 samples, although the spectral shapes are similar to Cr_2O_3, the shoulder is not as well defined. This suggests a modification of the primary Cr_2O_3 oxide structure in these samples.

Both Fe and Cr 2p spectra suggest a clear influence of the implanted ion species on the composition of the passive layer on the AISI 304 SS. The main effect produced by Si ion implantation is the formation of an outer layer composed mainly of Cr_2O_3 that should impart more stability and protection. On the contrary, Mo ion implantation seems to favor the formation of a passive layer composed of a mixture of Fe_3O_4, Fe_2O_3 and Cr_2O_3. The intermediate case is given by Ce ion implantation, which promotes the formation of a layer composed mainly of Cr_2O_3 with a modified structure and with small amounts of Fe oxides. Taking into account these results, it can be expected that the passive layer of the Mo-implanted sample, which is a mixture of Fe and Cr oxides, will be less protective than that of Ce and Si-implanted specimens.

The O 1s soft X-ray absorption spectra of the as-received and ion implanted AISI 304 samples as well as oxidized Cr and Fe reference materials are shown in Fig. 4. The O 1s XAS signal is the result of the electronic transitions into unoccupied states with O 2p character hybridized with metal states. Therefore, due to the presence of different oxides, the interpretation of these data is only qualitative. The oxygen spectra show two broad features. The first one, from 525 to 533 eV, corresponds to oxygen 2p states hybridized with 3d transition metal states. The second feature, from 533 to 545 eV, corresponds to oxygen 2p states hybridized with metal 4s and 4p states.

The O 1s signal of oxidized Cr exhibits a spectral profile that is rather similar to that of Cr_2O_3 [28] with small differences probably originated by the presence of OH groups in this sample. Additionally, the O 1s spectrum of oxidized Fe presents features which are similar to Fe_2O_3 and Fe_3O_4, suggesting a mixture of both oxides [28]. As in the oxidized Cr case, in this sample the presence of OH groups cannot be excluded. By comparing the O 1s spectral shapes of both reference materials, oxidized Cr and oxidized Fe, several differences can be noticed. The most evident distinction is that the photon energy position of the first spectral feature is located at lower energy values for oxidized Fe. Fig. 4 also exhibits the O 1s signals of the four AISI 304 samples showing spectral differences at the near-edge structure. Although the first feature (525–533 eV) is very similar in all AISI 304 samples, a distinctive shoulder marked by a vertical arrow appears in the case of the as-received and the

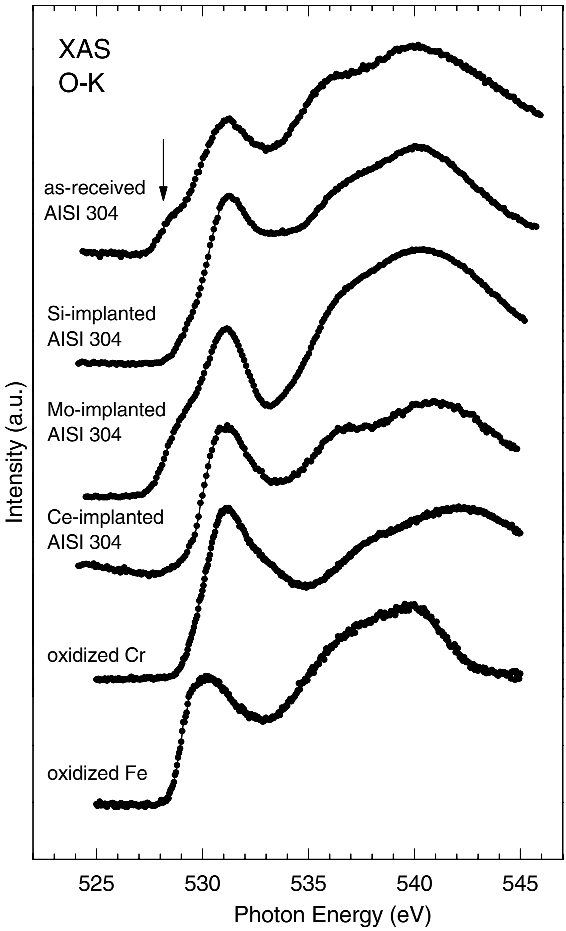

Fig. 4. O 1s soft X-ray absorption spectra of all AISI 304 SS samples: as-received and after Si, Mo, and Ce ion implantation, as well as oxidized Cr and oxidized Fe samples. The solid lines through the data points serve as a guide to the eyes.

Mo ion implanted AISI 304 samples. It is difficult to explain the presence of this shoulder in these two specimens. As it has been already mentioned, from Fig. 4 it can be observed that the onset of the oxidized iron peak appears at lower energies than that of oxidized chromium. Additionally, the Fe 2p spectra for Si and Ce ion implanted samples correspond mainly to metallic Fe, while that of as-received and Mo-implanted spectra exhibited important contributions of iron oxides. Taking into account these results and that the shoulder in the O 1s spectrum appears only for the as-received and Mo-implanted samples, its presence could be related to a higher content of iron–oxygen compounds in the passive layer of these samples. In the case of both Si and Ce ion implanted samples, their O 1s spectral profiles are similar to oxidized Cr, although the presence of small amounts of Fe compounds cannot be

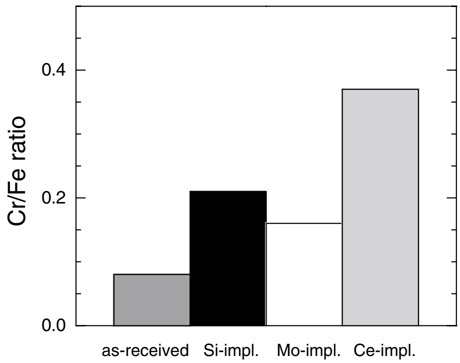

Fig. 5. Cr/Fe ratio for the as-received AISI 304 SS, and this material after Si, Ce and Mo ion implantation as obtained from the data of Fig. 1.

excluded. This result agrees with the Fe and Cr 2p spectra shown in Figs. 2 and 3 where the presence of mainly Cr_2O_3 with only small amounts of Fe oxides was observed.

The Cr/Fe ratio was calculated from the data of Fig. 1 for all AISI 304 samples and is represented in Fig. 5. Taking into account previous studies on the corrosion behavior of different materials, the Cr/Fe ratio is of great interest because a higher Cr content in the surface as compared to Fe usually indicates a higher corrosion resistance. Fig. 5 indicates that there is an increase of the Cr/Fe value for AISI 304 due to the ion implantation process, independent of the ion implanted element. Consequently, this figure suggests that the effect of performing an ion implantation process on the material is to increase Cr diffusion towards the surface, possibly due to the surface damage induced during the ion implantation process. This result agrees with previous work [29] where surface microstructural modifications induced by ion implantation on AISI 304 SS were detected. It was observed that Si, Ce and Mo ion implantation processes in this material give rise to a phase transformation (γ-austenite to α'-martensite) which causes an increase of the Cr diffusion coefficient. The Cr diffusion enhancement would result in an enhancement of the corrosion resistance of the material due to a more stable passive layer. Fig. 5 shows the highest Cr/Fe ratio for the Ce ion implanted sample. However, the Fe and Cr XAS spectra indicated that the passive layer on the Si ion implanted sample was composed mainly of Cr_2O_3 while the Ce ion implanted sample exhibited a passive layer with both Cr_2O_3 and small amounts of Fe compounds. The apparent disagreement between the XAS spectra and the highest Cr/Fe ratio for the Ce ion implanted sample can be explained by the formation of a stable passive layer of Cr_2O_3 for the Si ion implanted sample which is thinner than the passive layer of Ce ion implanted sample. This would give rise to a smaller Cr/Fe ratio for the Si ion implanted AISI 304 sample due, in this case, to a Fe signal coming also from the region below the passive layer. The result also agrees with the O 1s XAS spectrum for the Ce ion implanted sample, where the presence of Cr oxides in its passive layer was detected but not of Fe oxides. Thus, although the passive layer of the Ce ion implanted sample is probably formed not only by Cr_2O_3 but also by small amounts of Fe oxides, this sample has the highest Cr/Fe ratio because it has the thickest passive layer.

4. Conclusions

In order to obtain information on the chemical differences between the passive layer formed on AISI 304 SS before and after Si, Ce and Mo ion implantation, soft X-ray absorption spectra on AISI 304 samples, with and without ion implantation were obtained. The XAS technique is less surface sensitive than other conventional surface analysis techniques, like XPS or AES, and, therefore gives more information on the inner zone of the passive layer of SSs. Consequently, to evaluate the influence of different ion implantation processes on the passive layer of AISI 304 SS, the chemical properties of the passive layers were analyzed.

The differences observed in both the Fe and the Cr 2p XAS spectra show the influence of the ion implantation species on the composition of the passive layer on AISI 304 SS. Si ion implantation favors the formation of a passive layer composed mainly of Cr_2O_3. Ce ion implantation leads to the formation of a layer of mainly Cr_2O_3 with a modified structure and with small amounts of Fe oxides. Finally, Mo ion implantation results in the formation of a thin layer composed of a mixture of Fe_3O_4, Fe_2O_3 and Cr_2O_3.

The XAS spectra provide information on the percentage composition corresponding to the main elements of the outer layers. Thus, an enrichment of Cr in the ion implanted samples relative to the as-received AISI 304 has been observed. Additionally, Cr/Fe ratios suggest a thinner passive layer for the Si ion implanted sample than for the Ce ion implanted sample.

Acknowledgements

This work has been supported by the Spanish Interministerial Science and Technology Commission (CICYT) under Project MAT96-0917, and by the BESSY contract no. CHGE-CT93-0027 of the Human Capital and Mobility Program of the EU. Technical assistance by BESSY-staff is gratefully acknowledged.

References

[1] A.J. Sedriks, Corrosion of Stainless Steels, John Wiley, New York, 1979.
[2] D. Talbot, J. Talbot, Corrosion Science and Technology, CRC Press, New York, 1998, p. 253.
[3] R. Blumm, in: D. Coutsoradis, J.H. Davidson (Eds.), Materials for Advanced Power Engineering, Kluwer, 1994, p. 15.
[4] H. Kotschenreutter, in: D. Coutsoradis, J.H. Davidson (Eds.), Materials for Advanced Power Engineering, Kluwer, 1994, p. 31.
[5] S. Seal, S.K. Bose, S.K. Roy, Oxid. Met. 41 (1994) 139.
[6] Y. Saito, B. Önay, T. Maruyama, J. Phys. III 3 (1993) 217.

[7] R.J. Hussey, M.J. Graham, Oxid. Met. 45 (1996) 349.
[8] H.S. Isaacs, S.M. Huangs, J. Electrochem. Soc. 143 (1996) 277.
[9] X. de Buchere, P. Andreazza, C. Andreazza-Vignolle, C. Clinard, R. Erre, Surf. Coat. Tech. 80 (1996) 49.
[10] J. Stringer, Mater. Sci. Eng. 87 (1987) 1.
[11] P.Y. Hou, J. Stringer, Oxid. Met. 33 (1990) 357.
[12] A. Iskanderova, T.D. Radhabor, G.R. Rakhimova, Phys. Chem. Mech. Surf. 8 (1984) 1081.
[13] D. Duday, Ph.D. thesis, Universitéde La Rochette, France, 1998.
[14] M.F. Stroosnijder, J.D. Sunderkotter, M.J. Cristobal, H. Jenett, K. Isenbulgen, M.A. Baker, Surf. Coat. Tech. 83 (1996) 205.
[15] K. Asami, K. Hashimoto, S. Shimodaira, Corros. Sci. 18 (1978) 151.
[16] I. Olejford, H. Fischmeister, Corros. Sci. 15 (1975) 697.
[17] K. Asami, K. Hashimoto, S. Shimodaira, Corros. Sci. 16 (1976) 387.
[18] R. Kirchheim, B. Heine, H. Fischmeister, S. Hofmann, H. Knote, U. Stolz, Corros. Sci. 29 (1989) 899.
[19] Handbook of Auger Electron Spectroscopy, second ed., Physical Electronic Industries, Inc., Minnesota, 1976, pp. 1–16.
[20] M. Abbate, J.B. Goedkoop, F.M.F. De Groot, M. Grioni, J.C. Fuggle, S. Hofmann, H. Petersen, M. Sacchi, Surf. Interface Anal. 18 (1992) 65.
[21] S.L.M. Schroeder, Solid State Commun. 98 (1996) 405.
[22] S. Gota, M. Gautier-Soyer, M. Sacchi, Phys. Rev. B 62 (2000) 4187.
[23] J.M. Bastidas, M.F. López, A. Gutiérrez, C.L. Torres, Corros. Sci. 40 (1998) 431.
[24] M.F. López, A. Gutiérrez, C.L. Torres, J.M. Bastidas, J. Mater. Res. 15 (1999) 763.
[25] J.P. Biersack, L. Haggmark, Nucl. Instrum. Meth. 174 (1980) 257.
[26] J.F. Ziegler, J.P. Biersack, U. Littmark, The Stopping and Range of Ions in Solids, Pergamon Press, New York, 1985.
[27] L. Soriano, M. Abbate, F.M.F. De Groot, D. Alders, J.C. Fuggle, S. Hofmann, H. Petersen, W. Braun, Surf. Interface Anal. 20 (1993) 21.
[28] F.M.F. de Groot, M. Grioni, J.C. Fuggle, J. Ghijsen, G.A. Sawatzky, H. Petersen, Phys. Rev. B 40 (1989) 5715.
[29] F.J. Pérez, M.J. Cristobal, P. Hierro, F. Pedraza, Cyclic Oxidation of High Temperature Materials, Institute of Metals, London, 1999, p. 209.